SAND2020-2604C

Performance of Constitutive Models in Finite Element Analysis

William M. Scherzinger
Sandia National Laboratories

Abstract

Modeling the elastic-plastic response of metals is an important issue in a variety of industries. The ability to leverage existing and new material model functionality in engineering analysis relies upon practical considerations such as numerical integration, code implementation, verification, calibration, etc., with the requirement that models are implemented correctly and are not prohibitively expensive. A family of modular plasticity models have been implemented in the Sierra/SolidMechanics finite element code that allow for a wide range of yield surfaces, hardening models, and failure models. Assessments of model performance in assorted boundary value problems are presented to understand the tradeoffs between expensive, high fidelity simulations and lower fidelity simulations.

1 Introduction

Modeling of elastic-plastic behavior of metals is primarily done with the isotropic von Mises yield surface. However, many other yield surface models have been proposed in the literature for modeling a variety of behaviors, including anisotropic yield/flow and tension/compression asymmetry, which can provide increased fidelity for modeling and simulation. Implementation of these models in finite element codes has not been widespread due to the difficulty of their numerical implementation, but recent advances implementing robust return mapping algorithms [1, 2] have enabled their reliable implementation in solid mechanics codes.

In particular, the isotropic model of Hershey/Hosford [3] and the anisotropic models of Hill [4] and Barlat et. al. [5, 6] have been implemented in the Sierra/SolidMechanics code [7] at Sandia National Laboratories. In addition to these models, the isotropic and anisotropic models for tension/compression asymmetry by Cazacu, Plunkett, and Barlat [8] have also been implemented.

The implementation of these models is robust in that the integration of the models converges and they give accurate results. However, the performance of the models, i.e. their speed, is also of interest to analysts solving problems. Due to their complexity, the

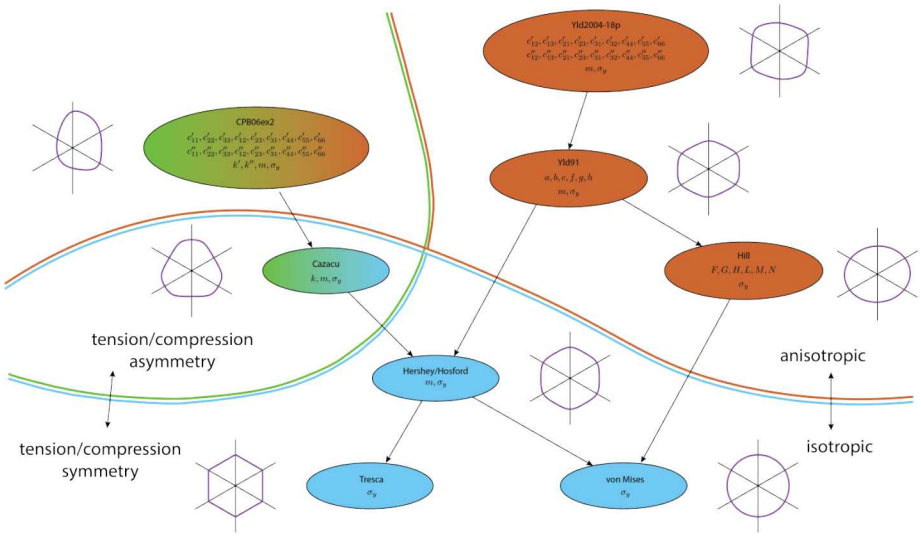

Figure 1: A family of yield surfaces with varying levels of fidelity.

models are naturally more expensive from a computational perspective. The goal of this work is to present problems that highlight the performance of these new yield surface models. Section 2 will describe the yield surface models used in this work. A test problem, uniaxial tension, will be presented in Section 3 along with results. Conclusions are presented in Section 4.

2 Yield Surface Models

In this work, attention is restricted to plasticity models that have a yield surface with associated plastic flow, encompassing the familiar isotropic models - von Mises and Tresca - along with models for anisotropy. The models implemented in Sierra/SolidMechanics are shown in Figure 1 and represent a family of yield surfaces. In this section, models will be divided into two groups: isotropic and anisotropic. Models for tension/compression asymmetry, while implemented in the finite element code, will not be presented in this work.

The plasticity models presented herein all have a yield surface definition with the following form

$$f\left(\boldsymbol{\sigma}, \bar{\varepsilon}^p\right) = \phi\left(\boldsymbol{\sigma}\right) - \bar{\sigma}\left(\bar{\varepsilon}^p\right) = 0 \tag{1}$$

where $\phi\left(\boldsymbol{\sigma}\right)$ is the effective stress, which we restrict to be a homogeneous function of degree one, and $\bar{\sigma}\left(\bar{\varepsilon}^p\right)$ is the flow stress which is a function of the equivalent plastic strain. The

yield surface shape, and whether it is isotropic or anisotropic, depends on the effective stress, $\phi(\boldsymbol{\sigma})$. The yield surface can also be made a function of temperature, although this will not be explicitly stated or examined in this work. Finally, behavior will be restricted to isotropic hardening; kinematic hardening and distortional hardening will not be considered here.

2.1 Isotropic Models

The simplest isotropic models, and the most commonly used, are the Tresca and von Mises models. The Tresca model, given by

$$\phi(\boldsymbol{\sigma}) = \frac{1}{2}\Big[|\sigma_1 - \sigma_2| + |\sigma_2 - \sigma_3| + |\sigma_3 - \sigma_1|\Big] \tag{2}$$

where σ_i are the principal stresses, is perhaps the simplest model and is often used for analytical calculations, but its implementation in finite element codes has not been widespread due to the difficulty of integrating the model for general loading paths. In contrast, the von Mises model, given by

$$\phi(\boldsymbol{\sigma}) = \sqrt{\frac{3}{2}\mathbf{s} : \mathbf{s}} \tag{3}$$

where $\mathbf{s}$ is the deviatoric stress, uses the radial return algorithm to numerically integrate the model. This has made that yield surface ubiquitous in finite element codes and it is the underlying yield surface for a large variety of plasticity models.

The Hershey/Hosford [3] model, defined as

$$\phi(\boldsymbol{\sigma}) = \left\{\frac{1}{2}\Big[|\sigma_1 - \sigma_2|^a + |\sigma_2 - \sigma_3|^a + |\sigma_3 - \sigma_1|^a\Big]\right\}^{1/a} \tag{4}$$

is another isotropic model that adds more flexibility in the response, where the exponent a allows for a more accurate representation of the shear or biaxial tension behavior for the material. Depending on the value of the exponent in the Hershey/Hosford model, a von Mises yield surface or a Tresca yield surface can be represented, or a yield surface that lies between these two. Both the Hershey/Hosford model and the tension/compression asymmetry model of Cazacu depend on calculating the eigenvalues and eigenvectors of the stress tensor to evaluate both yield and plastic flow. This is done in our code using the algorithm of Scherzinger and Dohrmann [9], which has been shown to be robust and efficient.

2.2 Anisotropic Models

Successful modeling of plastic deformation often requires modeling material anisotropy, and many choices are available for this. The most common model for anisotropy is Hill's model [4],

$$\begin{aligned}\phi^2(\boldsymbol{\sigma}) =& F(\hat{\sigma}_{22}-\hat{\sigma}_{33})^2 + G(\hat{\sigma}_{33}-\hat{\sigma}_{11})^2 + H(\hat{\sigma}_{11}-\hat{\sigma}_{22})^2 \\ &+ 2L\hat{\sigma}_{23}^2 + 2M\hat{\sigma}_{31}^2 + 2N\hat{\sigma}_{12}^2\end{aligned} \tag{5}$$

which is an extension for anisotropy of the quadratic von Mises model with F, G, H, L, M, and N model parameters. The model is generally capable of modeling anisotropic yield or flow, but often cannot accurately model both simultaneously. The models of Barlat and co-workers [5, 6] are parameterized in a way that provides flexibility to model both anisotropic yield and flow. The Yld91 model

$$\phi(\boldsymbol{\sigma}) = \left\{\frac{1}{2}\left[|s_1'-s_2'|^a + |s_2'-s_3'|^a + |s_3'-s_1'|^a\right]\right\}^{1/a} \quad ; \quad \mathbf{s}' = \mathbf{L}' : \boldsymbol{\sigma} \tag{6}$$

and Yld2004-18p model

$$\begin{aligned}\phi(\boldsymbol{\sigma}) =& \left\{\frac{1}{4}\Big[|s_1'-s_1''|^a + |s_1'-s_2''|^a + |s_1'-s_3''|^a + |s_2'-s_1''|^a + |s_2'-s_2''|^a \right. \\ &\left. + |s_2'-s_3''|^a + |s_3'-s_1''|^a + |s_3'-s_2''|^a + |s_3'-s_3''|^a\Big]\right\}^{1/a} \\ & \mathbf{s}' = \mathbf{L}' : \boldsymbol{\sigma} \quad ; \quad \mathbf{s}'' = \mathbf{L}'' : \boldsymbol{\sigma}\end{aligned} \tag{7}$$

where $\mathbf{L}'$ and $\mathbf{L}''$ are transformations whose components are model parameters. These models can be thought of as extensions of the Hershey/Hosford model for anisotropy where the anisotropy is encapsulated in a mapping of the stress state.

3 Analysis - Uniaxial Tension

The boundary value problem of a uniaxial tension specimen is used in this section to show the performance of these models. Two problems are examined. First, five models are

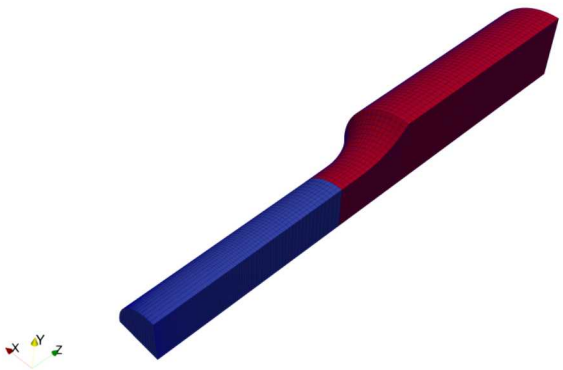

Figure 2: Finite element model for ASTM-E8 round bar tension specimen. The model has $1/8^{\text{th}}$ symmetry and contains 25,092 elements and 29,040 nodes. The gauge section is in blue.

parameterized so that they all reproduce a von Mises yield surface and used as the reference mdoel for this boundary value problem. Comparing these results gives a fair comparison of the increase in computational effort of progressively more complex models. Second, the five models are calibrated to the fit of the Yld2004-18p model parameterization for 2090-T3 Al given in Barlat et. al. [6]. These results show the cost not only of the algorithm, but also the effect of more complex models on both the integration of the constitutive model and the solution of the global boundary value problem.

The boundary value problem is a round bar uniaxial tension test based on the ASTM standard [10]. The finite element model uses $1/8^{\text{th}}$ symmetry and is shown in Figure 2. The mesh has 25,092 elements and 29,040 nodes. The model is loaded using displacement boundary conditions that target a nominal (engineering) strain rate of 0.001 to a final strain of 0.36. The actual strain is calculated using a virtual extensometer applied to the gauge section of the specimen. Since the boundary conditions are applied to the ends of the specimen, the strain rate and strain in the gauge section is less than the targets.

The elastic properties for the model are a Young's modulus, $E = 70$ GPa, and Poisson's ratio, $\nu = 0.33$. The initial yield stress is $\sigma_y = 197.2$ MPa and the hardening law is a rate-independent Voce model with a saturation stress of twice the initial yield stress, given by

$$\bar{\sigma}\left(\bar{\varepsilon}^p\right) = \sigma_y\left[2 - \exp\left(-b\bar{\varepsilon}^p\right)\right] \tag{8}$$

where $b = 5$ accounts for the hardening slope. This model is rate independent.

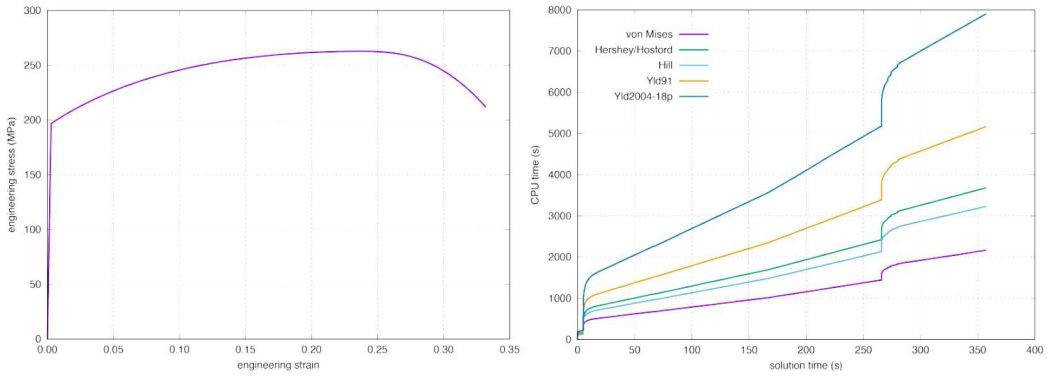

(a) (b)

Figure 3: The results for the uniaxial tension test analysis using the von Mises model showing (a) the engineering stress-strain curve, and (b) the timing for the five yield surface models.

3.1 von Mises Yield Surface

Five different yield surfaces will be tested - von Mises, Hershey/Hosford, Hill, Yld91, and Yld2004-18p - where they are parameterized so that they reproduce the von Mises yield surface, which is considered as the baseline model for the performance study. Examining the results compared to the von Mises model checks two things. First, is the numerical implementation of a model behaving exactly as we expect. Theoretically each model is parameterized as a von Mises yield surface, but the implementations are vastly different. The von Mises model uses a radial return algorithm, the Hill model uses a generalized line search algorithm, the Hershey/Hosford model adds an eigenvalue/eigenvector solver to the line search algorithm, and the Yld91 and Yld2004-18p models employ stress transformations, eigenvalue/eigenvector solves, and a line search algorithm. If the models give identical results, then timing studies can be used to understand the algorithmic cost of the higher fidelity models.

Figure 3a shows the engineering stress-strain curve calculated from the analysis, which was the same for all five yield surface models. Furthermore, when looking at the convergence behavior of the finite element model, the results for the five different models are the same. Each model took a total of 191 load steps and 875 iterations to solve the problem using an adaptive time stepping algorithm. Furthermore, on the last iteration of the last load step the residual calculated for each of the five models is the same, which is convincing evidence that all of the models, while implemented with vastly different algorithms, are behaving the same.

With identical behavior, the timing of each model can be examined to understand the computational costs of the integration algorithms used for each yield surface model. The

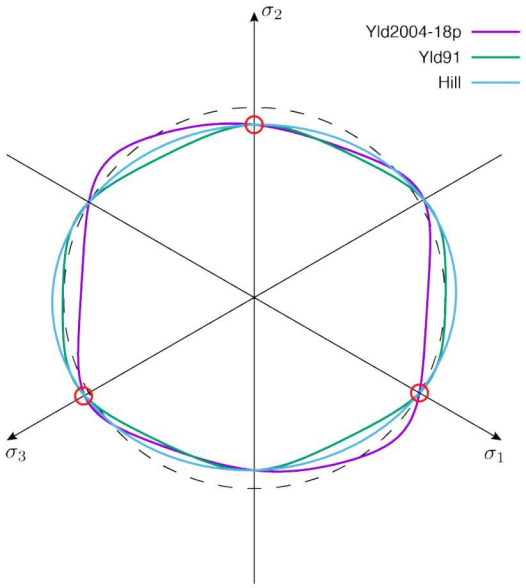

Figure 4: Three orthotropic yield surfaces for 2090 Al calibrated to the yield stress where the yield stress in the three principal material directions (red circles) is the same. An equivalent von Mises yield surface is given by the dotted line.

timing for each model is shown in Figure 3b. Increasing complexity results in a significant computational cost when compared to the baseline results of the von Mises model. The implementation of the Hill model is the least expensive and has a similar cost as the isotropic Hershey/Hosford model. The complexity of the Hill model comes in the calculations of the effective stress and flow directions, which assumes the material is orthotropic, whereas the complexity in the Hershey/Hosford model is in the eigenvalue/eigenvector calculations. The Yld91 and Yld2004-18p models are, understandably, the most expensive given the mappings of the stress state and the eigenvalue/eigenvector calculations. The Yld2004-18p model, using two mappings and two eigenvlaue/eigenvector calculations, is the most expensive model, and is almost four times as expensive as the von Mises model.

In addition to observations about relative model cost, the plot shows some distinct features of the solution. The initial solution requires some reductions in the time step to get started, hence the curves having a non-zero CPU time for zero solution time. A similar feature is seen at initial yield and at maximum load where the analysis has some difficulty with the change in the global solution resulting in time step cutbacks.

3.2 High Fidelity Yield Surfaces

The previous analysis is good for getting an apples-to-apples comparison of the efficiency of the model implementations. However, for real problems the performance of the material models and the finite element models will depend on the fidelity of the material model, which will be examined in this section.

The material is assumed to fit the Yld2004-18p parameterization for a 2090-T3 aluminum alloy given in [6]. If this material is assumed to be isotropic, two models are available: the von Mises and the Hershey/Hosford model. For both of these models the yield stress will be the yield stress in the x_1 material direction for the Yld2004-18p parameterization of 2090-T3 Al. Since the exponent on the Yld2004-18p parameterization is $a = 8$, this is the exponent that will be used with the Hershey/Hosford model. Three orthotropic models are also run: Hill, Yld91, and Yld2004-18p. The Hill and Yld91 models are fit to the yield stresses of the Yld2004-18p model for 2090-T3 Al. The yield surfaces, plotted in the π-plane for the three orthotropic models are shown in Figure 4 along with, for reference, the von Mises yield surface. As seen in the plots the yield in the three principal material directions is the same, but the flow direction, given by the normal to the yield surface, is different. Specifically the flow directions for the Hill and Yld91 models are very different from the flow direction for the Yld2004-18p model for uniaxial tension in the x_1 direction (the σ_1 axis) which is the direction of loading simulated in the uniaxial tension test. The models could be fit to the plastic flow, and yield in one direction, or some other combination of yield and flow, but for purposes of this work these cases are not examined. Every model has the same Voce hardening behavior in (8).

The results for the engineering stress-strain curves and the timing for each model are shown in Figure 5. The engineering stress-strain behavior is similar for every model up to maximum load. This is expected since the models have the same yield stress and hardening behavior. After maximum load the behavior differs, especially for the Yld2004-18p model. The load drop for the Yld2004-18p model is significantly greater than the load drop for any of the other models and is most likely due to the high degree of anisotropy in plastic flow that is captured by this model, but not by the other models.

The timing results in Figure 5b are similar to the results in Figure 3b for the isotropic models, but allow us to see the costs of model fidelity in addition to algorithmic costs. The von Mises model is the fastest; the Hershey/Hosford and Hill model results are comparable; the Yld91 model is slower and the Yld2004-18p model is the slowest. The plots also show the same three distinct regions corresponding to elastic deformation, uniform elongation after yield and before maximum load, and necking after maximum load. Prior to maximum load the timing looks linear for each model, with the slope increasing for models with increasing complexity. After maximum load, the more complex models, especially the orthotropic models, generally slow down even more as a result of the increasing complexity of the load paths and deformation patterns in the necked region. This can be seen in the Yld2004-18p model where, up to maximum load, the CPU time is approximately 6 times greater than

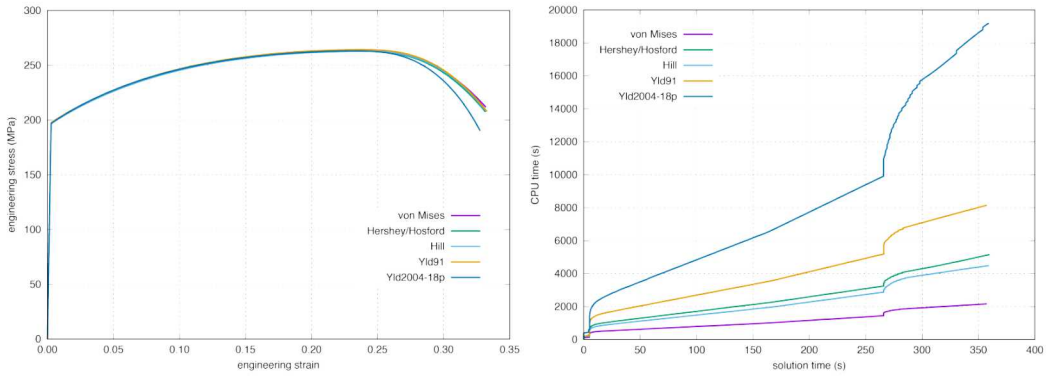

(a) (b)

Figure 5: The results for the uniaxial tension test analysis using the 2090-T3 Al parameterization for each model showing (a) the engineering stress-strain curves, and (b) the timing for each of the five yield surface models.

the von Mises model, but after maximum load the total CPU time is almost 10 greater.

4 Conclusions

Many choices are available for modeling plastic deformation in the Sierra/SolidMechanics finite element code. The performance of models with increasing levels of fidelity in the yield surface has been investigated in this work. With increasing fidelity comes increasing complexity which, when implemented in a finite element code, results in a performance hit in terms of CPU time. Knowing the relative costs of one model versus another allows computational cost to be included as a factor in modeling choices. However, while it is important to quantify performance costs in a finite element analysis, this is just one cost of using a higher fidelity model. It is also important to understand other costs associated with modeling, including calibration costs and model form error.

Calibration of complex yield surfaces requires a significant experimental effort, which is usually much greater than the computational cost. On the other hand, the cost of using a lower fidelity model that might miss important behaviors is another cost that must be considered. This work sets out an approach to quantify one cost for engineering analysis: the computational performance of high fidelity plasticity models. This approach to modeling provides a methodology for accounting for these costs in engineering analysis.

Sandia National Laboratories is a multimission laboratory managed and operated by National Technology and Engineering Solutions of Sandia, LLC., a wholly owned subsidiary

of Honeywell International, Inc., for the U.S. Department of Energy's National Nuclear Security Administration under contract DE-NA0003525.

References

[1] W. M. Scheriznger. A return mapping algorithm for isotropic and anisotropic plasticity models using a line search method. *Computer Methods in Applied Mechanics and Engineering*, 317:526–553, 2017.

[2] B. T. Lester and W. M. Scherzinger. Trust-region based return mapping algorithm for implicit integration of elastic-plastic constitutive models. *International Journal for Numerical Methods in Engineering*, 112:257–282, 2017.

[3] W. F. Hosford. A generalized isotropic yield criterion. *Journal of Applied Mechanics*, 39:607–609, 1972.

[4] R. Hill. A theory of the yielding and plastic flow of anisotropic metals. *Proceedings of the Royal Society of London: Series A.*, 193(1033):281– 297, 1948.

[5] F. Barlat, D. J. Lege, and J. C. Brem. A six-component yield function for anisotropic materials. *International Journal of Plasticity*, 7:693–712, 1991.

[6] F. Barlat, H. Aretz, J. W. Yoon, J. C. Brem, and R. E. Dick. Linear transformation-based anisotropic yield functions. *International Journal of Plasticity*, 21:1009–1039, 2005.

[7] SIERRA Solid Mechanics Team. Sierra/SM 4.52 User's Guide. SAND Report SAND2019-2715, Sandia National Laboratories, Albuquerque, NM and Livermore, CA, 2019.

[8] O. Cazacu, B. Plunkett, and F. Barlat. Orthotropic yield criterion for hexagonal closed packed metals. *International Journal of Plasticity*, 22:1171–1194, 2006.

[9] W. M. Scherzinger and C. R. Dohrmann. A robust algorithm for finding the eigenvalues and eigenvectors of 3×3 symmetric matrices. *Computer Methods in Applied Mechanics and Engineering*, 197:4007–4015, 2008.

[10] ASTM Standard E8/E8M-16a. Standard testing methods for tension testing of metallic materials. *ASTM International*, 2016.